

*Mini review*

## **Recent advancements in nanomaterials-based electrochemiluminescent and photoelectrochemical techniques for the determination of beta-amyloid peptides**

*Yunxiao Feng\* and Ming La\**

College of Chemistry and Chemical Engineering, Pingdingshan University, Pingdingshan, Henan 467000, People's Republic of China

\*E-mail: [2743@pdsu.edu.cn](mailto:2743@pdsu.edu.cn) (Y.F.); [mingla2011@163.com](mailto:mingla2011@163.com) (M.L.)

*Received: 2 December 2021 / Accepted: 19 December 2021 / Published: 5 January 2022*

---

Beta-amyloid (A $\beta$ ) peptides have been considered as the core biomarkers for early diagnosis of Alzheimer's disease. Electrochemiluminescent (ECL) and photoelectrochemical (PEC) biosensors are two promising methods for disease diagnosis in view of their merits of high sensitivity, low-cost and broad dynamic response range. In this review, we summarized the development of ECL and PEC biosensors for the sensitive analysis of A $\beta$  species.

---

**Keywords:** electrochemiluminescence; photoelectrochemistry; nanomaterials; Alzheimer's disease; beta-amyloid peptides

### **1. INTRODUCTION**

Alzheimer's disease (AD), a common chronic neurodegenerative disease, is characterized by memory decline, decreased language and direction ability, loss of mobility and thinking, and behavior disorders. Studies in recent years have demonstrated that there are two classical clinical biomarkers, including extracellular accumulation of beta-amyloid (A $\beta$ ) peptides in senile plaques and neurofibrillary tangles (NFTs) [1, 2]. The neurotoxic A $\beta$  peptides are produced by the cleavage of amyloid precursor protein (APP) and generally consist of 39-43 amino acids. They can cause neuronal dysfunction and induce neuronal apoptosis by interacting with cell surface receptors. In addition, the peptides have a tendency to aggregate at different stages, and the process is affected by many aspects, including pH, temperature, peptide concentration, and intermolecular interactions. A $\beta$  peptides can form soluble A $\beta$  oligomers (A $\beta$ O) through aggregation and spatial folding, and then form fibrous amyloid. These aggregates can cause oxidative damage to DNA and protein, and gradually lead to synaptic dysfunction, inflammation, and phenomena such as neuron loss. Thus, A $\beta$  peptides and their aggregates during the

progressive aggregation process have been considered as the core biomarkers for early diagnosis of AD [3-5].

To date, great efforts have been given to develop effective platforms and devices for accurate and sensitive detection of A $\beta$  species, including mass spectrometry (MS), fluorescence, colorimetric assay, surface-enhanced Raman scattering, electrochemical technique and so forth [6-18]. However, those methods exhibit some disadvantages, such as low sensitivity, costly instrument and time-consuming procedure. Among them, electrochemiluminescent (ECL) and photoelectrochemical (PEC) biosensors are two promising methods because of their merits of high sensitivity, low-cost and broad dynamic response range [19]. Moreover, the distinct form of excitation source and detection signal endow them with excellent advantages of the significantly reduced background signal and high signal-to-noise ratio. Therefore, they have been widely applied in the fields of disease diagnosis, drug research, food safety and environment monitoring. More importantly, due to the prosperous development of nanotechnology, many novel nanomaterials have been applied in the construction of new and powerful detection platforms, remarkably improving the analytical detection performances [20]. In this review, we summarized and addressed the development of ECL and PEC biosensors for the sensitive analysis of A $\beta$  species. The role and importance of nanomaterials in the fabrication of biosensors were discussed.

## 2. ECL BIOSENSORS

During the past decades, ECL method has becoming an attractive technique for A $\beta$  detection because it combine the advantages of electrochemical and optical techniques, such as low background signal, excellent sensitivity, simple instrumentation, and extensive dynamic range. The reagents used for the development of ECL sensing strategies include Ru(bpy) $_3^{2+}$ , luminol, quantum dots (QDs) and so on (Table 1) [21]. For example, Qin et al. reported a label-free ECL aptasensor for A $\beta$ (1-16) monomer detection using luminol as the ECL luminophor [22]. In this study, A $\beta$ (1-16) monomer could bind with Cu $^{2+}$  ion and catalyze the in-situ generation of reactive oxygen species (ROS) from dissolved O $_2$  in the presence of ascorbic acid (AA). The produced ROS could enhance the generation of the excited luminol for emission improvement. Nanomaterials with enzyme-like properties (nanozymes) have been broadly applied in ECL bioassays because they can catalyze the decomposition of H $_2$ O $_2$  to produce large amounts of ROS [23]. For this view, Wang et al. fabricated a nanomaterial-enhanced luminol-based sandwich-type ECL immunosensor for A $\beta$  detection [24]. As shown in Figure 1, protein-like silver-cysteine nanowires (AgCys NWs) were prepared and utilized to modify the gold deposited glass carbon electrode (GCE) for the assembly of primary antibody (Ab $_1$ ). Ceria-doped ZnO nanoflowers (Ce:ZONFs) were synthesized in the presence of lysine. Then, luminol, anti-A $\beta$  (Ab $_2$ ) and glucose oxidase (GOD) molecules were successively bound to the surface of nanoflowers through amidation and physical adsorption. H $_2$ O $_2$  from the catalytic reaction between GOD and glucose could be converted into ROS under the catalysis of Ce:ZONFs and enhance the emission of luminol. Moreover, the fast Ce $^{4+}$   $\leftrightarrow$  Ce $^{3+}$  transformation could accelerate the electron-transfer rate and improve the ECL emission significantly. This method achieved a relatively low limit of detection (LOD) (52 fg/mL) and a wide linear range from 52 fg/mL to 100 ng/mL.

**Table 1** Analytical performances of different ECL biosensors for detection of A $\beta$  species.

Signal label	Target	LOD	Linear range	Ref.
A $\beta$ -Cu <sup>2+</sup> complex	A $\beta$ (1-16) monomer	0.035 pg/mL	1 $\times$ 10 <sup>-4</sup> – 10 ng/mL	[22]
AuNP/Fe-MIL-88NH <sub>2</sub> MOF	A $\beta$ (1-42) oligomer	71.0 fM	0.1 - 10 pM	[23]
Ce:ZONFs-luminol	A $\beta$ monomer	0.052 pg/mL	5.2 $\times$ 10 <sup>-5</sup> – 100 ng/mL	[24]
g-C <sub>3</sub> N <sub>4</sub> -heme	A $\beta$ (1-40)	0.00325 pg/mL	1 $\times$ 10 <sup>-5</sup> – 100 nM	[25]
AgNCs-TiO <sub>2</sub> NFs	A $\beta$ monomer	0.032 pg/mL	5 $\times$ 10 <sup>-5</sup> – 100 ng/mL	[26]
MnCO <sub>3</sub> nanospheres	A $\beta$ (1-42) oligomer	0.01995 pg/mL	1 $\times$ 10 <sup>-4</sup> – 10 ng/mL	[27]
luminol@SnS <sub>2</sub> -Pd and Cu:WO <sub>3</sub> -AuNPs	A $\beta$ (1-42) monomer	0.0054 pg/mL	1 $\times$ 10 <sup>-4</sup> – 50 ng/mL	[28]
CuS@CoS <sub>2</sub> DSNBs@AgNPs/AuNPs@C <sub>3</sub> N <sub>4</sub>	A $\beta$ (1-42) oligomer	0.0038 pg/mL	5 $\times$ 10 <sup>-4</sup> – 20 ng/mL	[29]
MOCs/nafion/Ru(bpy) <sub>3</sub> <sup>2+</sup> and GNRs	A $\beta$ (1-40) monomer	0.0042 pg/mL	1 $\times$ 10 <sup>-5</sup> – 100 ng/mL	[30]
Zinc oxalate MOFs/Au@NiFe MOFs	A $\beta$ monomer	0.0138 pg/mL	1 $\times$ 10 <sup>-4</sup> – 50 ng/mL	[31]
NH <sub>2</sub> -UiO-66/MIL-101@Au-MoS <sub>2</sub> QDs	A $\beta$ monomer	0.00332 pg/mL	1 $\times$ 10 <sup>-5</sup> – 50 ng/mL	[32]
luminol-Au@MoS <sub>2</sub> /Bi <sub>2</sub> S <sub>3</sub>	A $\beta$ (1-42)	0.021 pg/mL	5 $\times$ 10 <sup>-5</sup> – 10 ng/mL	[33]
Ru@MOF and g-C <sub>3</sub> N <sub>4</sub>	A $\beta$ monomer	0.0039 pg/mL	1 $\times$ 10 <sup>-5</sup> – 500 ng/mL	[34]

Abbreviation: MOF: metal organic framework; Ce:ZONFs: ceria doped ZnO nanoflowers; AgNCs-TiO<sub>2</sub> NFs: silver nanoclusters/titanium oxide nanoflowers; AuNPs; gold nanoparticles; DSNBs: double shelled nanoboxes; AgNPs: silver nanoparticles; MOCs: mesoporous carbon nanospheres; GNRs: gold nanorods; QDs: quantum dots; Ru@MOF: Ru(bpy)<sub>3</sub><sup>2+</sup>-loaded MOFs.

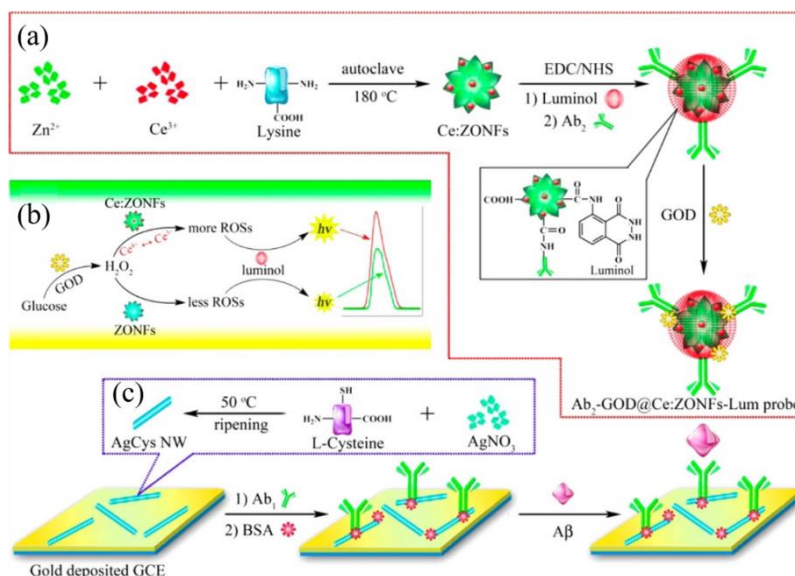


**Figure 1.** Schematic representation of preparation of synthesis process of Ab<sub>2</sub>-GOD@Ce:ZONFs-Lum signal probe (a); Possible ECL mechanism of signal generation and enhancement (b); Preparation process of the AgCys nanowires (c) [24]. Copyright 2016 American Chemical Society.

Nowadays, many types of nanomaterials have been reported to possess ECL properties and used as ECL labels for establishing novel platforms for biosensing and bioimaging. To overcome the

shortcoming of low luminous intensity, different co-reactants and accelerators have been explored and introduced into the solution. For example, Zhang et al. demonstrated that g-C<sub>3</sub>N<sub>4</sub>-heme could be labeled with the captured A $\beta$  by the formation of a heme-A $\beta$  complex and g-C<sub>3</sub>N<sub>4</sub> could produce dual-enhanced ECL signal with the in-situ generated H<sub>2</sub>O<sub>2</sub> and original K<sub>2</sub>S<sub>2</sub>O<sub>8</sub> as co-reactants [25]. Zhou et al. developed a ferrocene (Fc)-modulated light switch biosensor for the detection of A $\beta$  by using silver nanoclusters (AgNCs)/titanium oxide nanoflowers (TiO<sub>2</sub> NFs) as the signal probes [26]. As shown in Figure 2A, TiO<sub>2</sub> NFs were functionalized with bovine serum albumin (BSA) for in-situ synthesis of AgNCs. More importantly, TiO<sub>2</sub> NFs with highly effective area accelerated the reduction of dissolved O<sub>2</sub> into OH<sup>•</sup> that could in-situ promote the generation of excited-state species Ag NCs\* and amplify the ECL signal. However, Fc molecules in the dsDNA strands may consume ROS and quench the ECL of AgNCs. To improve the sensitivity of the double-antibody immunoassay, Exo III-driven DNA-based amplification strategy was integrated into this method. Minute A $\beta$  proteins were converted into numerous secondary-target DNA products and thus resulted in the release of abundant Fc molecules, leading to the obvious recovery of ECL signal. MnCO<sub>3</sub> was demonstrated to show high ECL efficiency with the aid of K<sub>2</sub>S<sub>2</sub>O<sub>8</sub> and has great potential in ECL bioassays due to its excellent biocompatibility and low toxicity. Jia et al. employed MnCO<sub>3</sub> nanospheres as the novel ECL emitters to construct an immunosensor for the detection of A $\beta$ (1-42) oligomers (Figure 2B) [27]. In this work, polydimethyldiallylammonium chloride (PDDA) and AuNPs were adsorbed on the surface of MnCO<sub>3</sub> (MnCO<sub>3</sub>/PDDA/Au) via the electrostatic interactions. For site-directed antibody fixation and better maintaining of the antibody activity, the HWRGWVC (HC-7) heptapeptide was used for the immobilization of antibodies on the MnCO<sub>3</sub>/PDDA/Au. With the increasing concentrations of A $\beta$ (1-42), the nonconductivity of peptides hindered the electron transfer and induced the decrease of ECL intensities. The immunosensor exhibited a favorable detection result toward A $\beta$ (1-42) in the range of 0.1 pg/mL to 10 ng/mL with an ultralow LOD of 19.95 fg/mL.

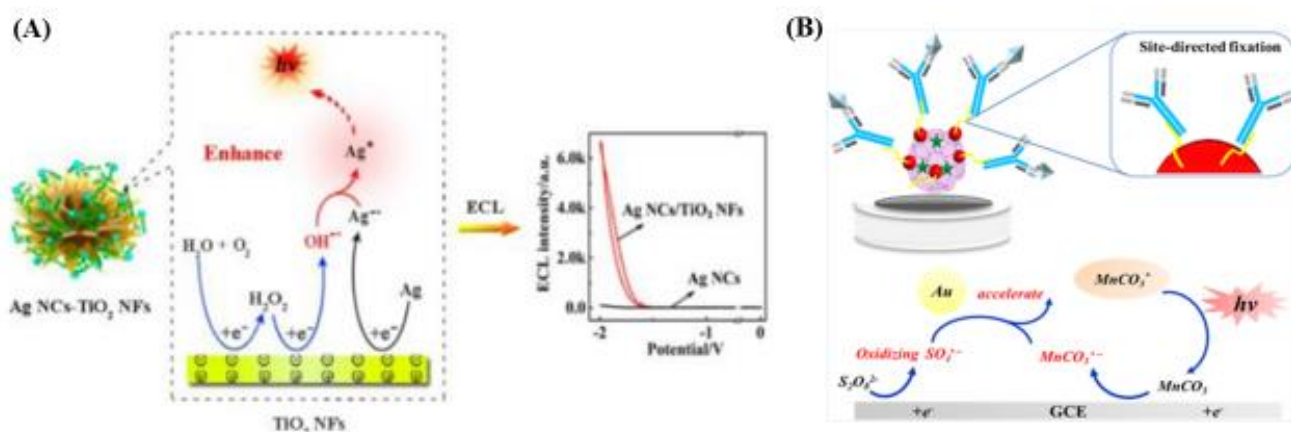


**Figure 2.** (A) Schematic representation and possible ECL emitting mechanism of AgNCs-TiO<sub>2</sub> NFs [26]. Copyright 2017 American Chemical Society. (B) Schematic representation of MnCO<sub>3</sub> nanospheres as a novel ECL emitter for immunosensor [27]. Copyright 2019 American Chemical Society.

ECL resonance energy transfer (ECL-RET) can be used to develop versatile quench-type detection platforms with high sensitivity [28, 29]. The technique plays an important role to select the energy donor and acceptor with critical matching between ECL emission spectrum and absorption spectrum, respectively. For instance, Ke et al. suggested that gold nanorods (GNRs) with a local surface plasmon resonance (LSPR) absorption peak at about 650 nm could effectively modulate the ECL emission of classical  $\text{Ru}(\text{bpy})_3^{2+}$  molecules through ECL-RET. This phenomenon was used to develop a sensing platform for the detection of  $\text{A}\beta(1-40)$  [30]. Moreover, Zhao et al. proposed dual-quenching ECL strategy for the detection of  $\text{A}\beta$  [31]. As illustrated in Figure 3A, zinc oxalate metal-organic frameworks (MOFs) were used to in-situ loading of ECL chromophore  $\text{Ru}(\text{bpy})_3^{2+}$  and capture antibody ( $\text{Ab}_1$ ). The three-dimensional channel could protect chromophores from solvent molecules and enhance the ECL emission efficiency. AuNPs and NiFe MOFs in  $\text{Au@NiFe}$  MOFs nanocomposites could quench the ECL of  $\text{Ru}(\text{bpy})_3^{2+}$  in MOFs ( $\text{Ru@MOFs}$ ) through ECL-RET, resulting in the significant improvement of sensitivity. Meanwhile, besides ECL-RET effect, nanoquenchers can also competitively consume co-reactants to further decrease the ECL intensity [32]. For instance, Li et al. reported that curcumin-conjugated ZnO NPs could quench the ECL of lumimol on  $\text{Au@MoS}_2/\text{Bi}_2\text{S}_3$  nanorods through ECL-RET and competitive consumption of  $\text{O}_2^-$  [33]. Single signal mode (especially signal-off mode) always confronts of false positive signal. To avoid this problem, Wang et al. designed a ratiometric ECL aptasensor for  $\text{A}\beta$  detection by using  $\text{g-C}_3\text{N}_4$  and  $\text{Ru@MOF}$  as the energy donor-receptor pair [34]. As displayed in Figure 3B,  $\text{Ru@MOFs}$  were synthesized through one-pot method and their absorption spectrum was overlapped largely with the ECL spectrum of  $\text{g-C}_3\text{N}_4$ , leading to the decrease of ECL signal of  $\text{g-C}_3\text{N}_4$  via ECL-RET. Furthermore, 2-amino terephthalic acid in  $\text{Ru@MOFs}$  could act as a co-reactant accelerator to enhance the ECL intensity of  $\text{Ru@MOFs}$ . Based on the ratio of  $\text{ECL}_{460\text{nm}}/\text{ECL}_{620\text{nm}}$ ,  $\text{A}\beta$  was sensitively detected in the range of 10 fg/mL to 500 pg/mL with a LOD of 3.9 fg/mL.

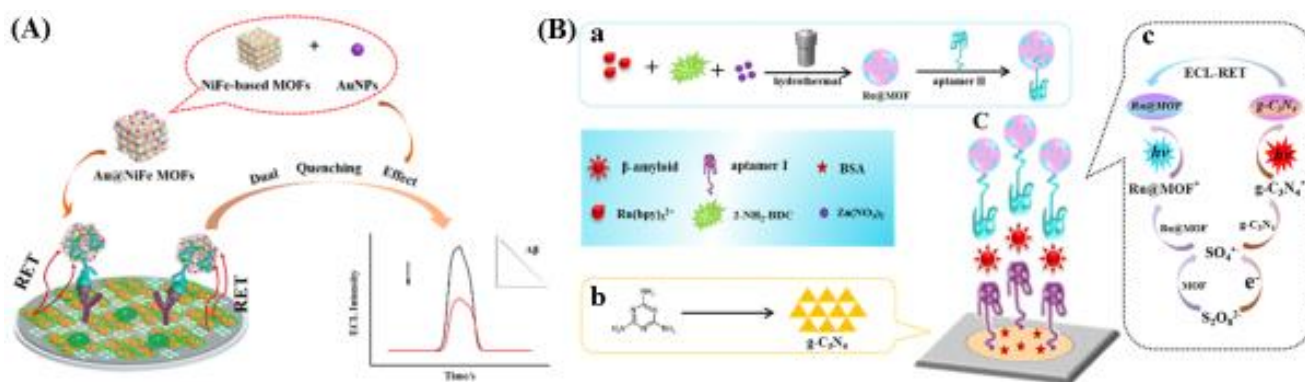


**Figure 3.** (A) Schematic representation and construction process of the proposed dual-quenching ECL immunosensor [31]. Copyright 2019 American Chemical Society. (B) Schematic representation of synthesis of aptamer II– $\text{Ru@MOF}$  signal probe (a); Fabrication process of  $\text{g-C}_3\text{N}_4$  NS (b); Construction procedure of the dual-wavelength ratiometric ECL sensor (c); and possible detection mechanism (d) [34]. Copyright 2019 American Chemical Society.

### 3. PEC BIOSENSORS

Since many photosensitive inorganic and organic materials have been discovered for converting the excitation light into electrical signal, PEC biosensors based on photoelectric effect have attracted increasing attention in recent years. It is popular to couple a wide band gap semiconductor with two or more small band gap sensitizers to promote the photocurrent conversion efficiency. Direct PEC detection of A $\beta$  is mainly dependent on the insulating A $\beta$  peptide-induced blocking of the access of electron donor reagent to photoactive matrix for scavenging photogenerated holes to suppress e<sup>-</sup>/h<sup>+</sup> recombination (Table 2) [35-37]. For example, Zhang et al. reported a PEC immunosensor for direct detection of A $\beta$  using CdS/CdTe-cosensitized SnO<sub>2</sub> [38]. For sensitive detection of low concentrations of targets, nanomaterials-based signal amplification strategies are introduced into the PEC sensing protocols. Generally, nanomaterials can be used as signal nanoquenchers through the competitively light energy harvesting and electron donor consuming effect [39]. For example, Fan et al. reported a sandwich-type PEC immunosensor based on dual-inhibited polystyrene@CuS (PS@CuS) nanocomposites [40]. In this study, CuS could not only act as a competitor of light energy to hinder the light to the photoactive matrix, but also consume AA to decrease the holes scavenging efficiency, resulting in the declined photocurrents. Moreover, the non-conductive PS also enhanced the steric hindrance of the sensing electrode and blocked the electron transfer from AA to the matrix.

In contrast to the “signal-on” amplification methods, “signal-off” strategies are more popular because of their higher sensitivity and selectivity. Due to the fast recombination of photo-generated electron-hole (e<sup>-</sup>/h<sup>+</sup>) pairs, bismuth tungstate (Bi<sub>2</sub>WO<sub>6</sub>) is rarely used in the PEC field. Xu et al. reported that Mn<sup>2+</sup>-doped CdSe NPs could induce the generation of energy defect, suppress the recombination of photo-generated e<sup>-</sup>/h<sup>+</sup> pairs and dramatically increase PEC signal [41]. Based on this phenomenon, A $\beta$  was sensitively analyzed by a competitive PEC immunosensor. For example, Feng et al. reported the “signal-on” PEC detection of A $\beta$  by employing core-shell CdSe@CdS QDs sensitized GO as the amplification label [42].

**Table 2.** Analytical performances of different PEC biosensors for detection of A $\beta$  species.

Signal label	Target	LOD	Linear range	Ref.
Zn:SnO <sub>2</sub> /SnS <sub>2</sub> -AuNPs	A $\beta$ monomer	0.05 pg/mL	1 × 10 <sup>-4</sup> – 100 ng/mL	[35]
SnO <sub>2</sub> /CdCO <sub>3</sub> /CdS	A $\beta$ monomer	0.05 pg/mL	1 × 10 <sup>-4</sup> – 100 ng/mL	[36]
SnO <sub>2</sub> /SnS <sub>2</sub> /Ag <sub>2</sub> S	A $\beta$ monomer	0.17 pg/mL	5 × 10 <sup>-5</sup> – 100 ng/mL	[37]
SnO <sub>2</sub> /CdS/CdTe	A $\beta$ monomer	0.18 pg/mL	5 × 10 <sup>-4</sup> – 10 ng/mL	[38]
PbS-AuNPs and TiO <sub>2</sub> /BiOI	A $\beta$ monomer	0.028 pg/mL	1 × 10 <sup>-4</sup> – 500 ng/mL	[39]
Ce-CdS and PS@CuS	A $\beta$ monomer	0.37 pg/mL	1 × 10 <sup>-3</sup> – 100 ng/mL	[40]
Bi <sub>2</sub> WO <sub>6</sub> /CdS and Mn:CdSe	A $\beta$ (1-42) monomer	0.068 pg/mL	200 – 50 ng/mL	[41]
GO/CdSe@CdS QDs and AuNPs/ $\alpha$ -Fe <sub>2</sub> O <sub>3</sub>	A $\beta$ monomer	0.02 pg/mL	6 × 10 <sup>-5</sup> – 350 ng/mL	[42]
CuO/g-C <sub>3</sub> N <sub>4</sub> and MoS <sub>2</sub> QDs@Cu NWs	A $\beta$ oligomer	5.79 fM	10 fM – 0.5 $\mu$ M ng/mL	[43]

Abbreviation: AuNPs: gold nanoparticles; PS: polystyrene; GO: graphene oxide; QDs: quantum dots.



Nanozymes have also been employed in PEC sensing system. For example, Zhang et al. used MoS<sub>2</sub> QDs@Cu nanowires (NWs) as the multifunction signal amplifiers to develop a “on-off-on” PEC aptasensor [43]. In this work, Cu NWs could not only enhance the activity of MoS<sub>2</sub> QDs nanozymes, but also suppress recombination of e<sup>-</sup>/h<sup>+</sup> pairs. MoS<sub>2</sub> QDs@Cu NWs catalyzed the precipitation of benzo-4-chlorohexadienone (4-CD) on the electrode surface and resulted in the decrease of photocurrent. In the presence of A $\beta$ , the stronger binding between aptamer and A $\beta$  promoted the dissociation of dsDNA and then nanozymes were released from the electrode. As a result, less precipitation was generated and the photocurrent was recovered.

#### 4. CONCLUSION

In this review, we mainly summarized the ECL and PEC biosensors as potential tools for the detection of A $\beta$  species through the comprehensively introduction of nanomaterials-based signal amplification. In spite of their tremendous advance, several existing obstacles and challenges should be resolved for subsequently practical applications. For example, during the manufacturing procedures, the stability and reproducibility of the modified electrodes and nanomaterials should be improved. Portable sensing devices with high detection performance should be developed to meet the need of reduced cost and increased commercialization.

#### ACKNOWLEDGMENTS

This work was supported by the National Natural Science Foundation of China (U2004193).

#### References

1. J. Hardy and D. J. Selkoe, *Science*, 297 (2002) 353.
2. C. Janus, J. Pearson, J. McLaurin, P. M. Mathews, Y. Jiang, S. D. Schmidt, M. A. Chishti, P. Horne, D. Heslin, J. French, H. T. Mount, R. A. Nixon, M. Mercken, C. Bergeron, P. E. Fraser, P. St George-Hyslop and D. Westaway, *Nature*, 408 (2000) 979.
3. A. Jamerlan, S. S. A. An and J. Hulme, *TrAC-Trend Anal. Chem.*, 129 (2020) 115919.
4. Y. Zhang, B. Ren, D. Zhang, Y. Liu, M. Zhang, C. Zhao and J. Zheng, *J. Mater. Chem. B*, 8 (2020) 6179.
5. L. Liu, Y. Chang, J. Yu, M. Jiang and N. Xia, *Sens. Actuat. B: Chem.*, (2017) 359.
6. E. J. Blackie, E. C. Le Ru and P. G. Etchegoin, *J. Am. Chem. Soc.*, 131 (2009) 14466.
7. W. K. Fang, L. Liu, L. L. Zhang, D. Liu, Y. Liu and H. W. Tang, *Anal. Chem.*, 93 (2021) 12447.
8. T. Hu, S. Lu, C. Chen, J. Sun and X. Yang, *Sens. Actuat. B: Chem.*, 243 (2017) 792.
9. M. Korecka and L. M. Shaw, *J. Neurochem.*, 159 (2021) 211.
10. H. Li, Y. Cao, X. Wu, Z. Ye and G. Li, *Talanta*, 93 (2012) 358.
11. S. Li and K. Kerman, *Biosens. Bioelectron.*, 179 (2021) 113035.
12. E. Mikula, *Curr. Med. Chem.*, 28 (2021) 4049.
13. L. M. T. Phan, T. X. Hoang, T. A. T. Vo, H. L. Pham, H. T. N. Le, S. R. Chinnadayya, J. Y. Kim, S. M. Lee, W. W. Cho, Y. H. Kim, S. H. Choi and S. Cho, *Expert Rev. Mol. Diagn.*, 21 (2021) 175.
14. M. Schaier, G. Hermann, G. Koellensperger and S. Theiner, *Anal. Bioanal. Chem.*, (2021) DOI: 10.1007/s00216-00021-03571-00216.
15. V. Serafin, M. Gamella, M. Pedrero, A. Montero-Calle, C. A. Razzino, P. Yanez-Sedeno, R.

- Barderas, S. Campuzano and J. M. Pingarron, *J. Pharm. Biomed. Anal.*, 189 (2020) 113437.
16. N. Xia, Y. Chang and Y. Hao, *Int. J. Electrochem. Sci.*, 12 (2017) 6255.
  17. Y. Xing, X. Feng, L. Zhang, J. Hou, G. Han and Z. Chen, *Int. J. Nanomed.*, 12 (2017) 3171.
  18. N. Xia, B. Zhou, N. Huang, M. Jiang, J. Zhang and L. Liu, *Biosens. Bioelectron.*, 85 (2016) 625.
  19. M. La, C. Chen, X. Xia, J. Zhang and B. Zhou, *Int. J. Electrochem. Sci.*, 14 (2019) 5547.
  20. C. Toyos-Rodriguez, F. J. Garcia-Alonso and A. de la Escosura-Muniz, *Sensors*, 20 (2020) 4748.
  21. H. Liu, X. Zhou, Q. Shen and D. Xing, *Theranostics*, 8 (2018) 2289.
  22. H. Qin, X. Gao, X. Yang, W. Cao and S. Liu, *Biosens. Bioelectron.*, 141 (2019) 111438.
  23. L. Yin, Y. Wang, R. Tan, H. Li and Y. Tu, *Microchim. Acta*, 188 (2021) 53.
  24. J. X. Wang, Y. Zhuo, Y. Zhou, H. J. Wang, R. Yuan and Y. Q. Chai, *ACS Appl. Mater. Inter.*, 8 (2016) 12968.
  25. M. Zhang, Z. Chen, H. Qin, X. Yang, W. Cao and S. Liu, *Electrochim. Acta*, 361 (2020) 137096.
  26. Y. Zhou, H. Wang, Y. Zhuo, Y. Chai and R. Yuan, *Anal. Chem.*, 89 (2017) 3732.
  27. Y. Jia, L. Yang, R. Feng, H. Ma, D. Fan, T. Yan, R. Feng, B. Du and Q. Wei, *ACS Appl. Mater. Inter.*, 11 (2019) 7157.
  28. J. Xue, L. Yang, H. Wang, T. Yan, D. Fan, R. Feng, B. Du, Q. Wei and H. Ju, *Biosens. Bioelectron.*, 133 (2019) 192.
  29. A. Ali, J. Zhao, M. S. Khan, H. Wang, X. Ren, L. Hu, R. Manzoor, D. Wu and Q. Wei, *Sens. Actuat. B: Chem.*, 329 (2021) 129155.
  30. H. Ke, H. Sha, Y. Wang, W. Guo, X. Zhang, Z. Wang, C. Huang and N. Jia, *Biosens. Bioelectron.*, 100 (2018) 266.
  31. G. Zhao, Y. Wang, X. Li, Q. Yue, X. Dong, B. Du, W. Cao and Q. Wei, *Anal. Chem.*, 91 (2019) 1989.
  32. X. Dong, G. Zhao, X. Li, J. Fang, J. Miao, Q. Wei and W. Cao, *Talanta*, 208 (2020) 120376.
  33. X. Li, D. Wu, H. Ma, H. Wang, Y. Wang, D. Fan, B. Du, Q. Wei and N. Zhang, *Biosens. Bioelectron.*, 131 (2019) 136.
  34. Y. Wang, Y. Zhang, H. Sha, X. Xiong and N. Jia, *ACS Appl. Mater. Inter.*, 11 (2019) 36299.
  35. N. Gao, Y. Zhang, K. Gao, J. Xie, L. Liu, Y. Li, L. Qiu, Q. Wei, H. Ma and X. Pang, *Sens. Actuat. B: Chem.*, 308 (2020) 127576.
  36. Y. Zhang, M. Wang, Y. Wang, J. Feng, Y. Zhang, X. Sun, B. Du and Q. Wei, *Biosens. Bioelectron.*, 126 (2019) 23.
  37. Y. Wang, D. Fan, G. Zhao, J. Feng, D. Wei, N. Zhang, W. Cao, B. Du and Q. Wei, *Biosens. Bioelectron.*, 120 (2018) 1.
  38. N. Zhang, Y. Wang, G. Zhao, C. Wang, Y. Li, Y. Zhang, H. Wang and Q. Wei, *Analyst*, 145 (2020) 619.
  39. Q. Han, H. Chi, H. Wang, D. Wu and Q. Wei, *Anal. Chim. Acta*, 1092 (2019) 85.
  40. D. Fan, X. Liu, C. Bao, J. Feng, H. Wang, H. Ma, D. Wu and Q. Wei, *Biosens. Bioelectron.*, 129 (2019) 124.
  41. R. Xu, D. Wei, B. Du, W. Cao, D. Fan, Y. Zhang, Q. Wei and H. Ju, *Biosens. Bioelectron.*, 122 (2018) 37.
  42. J. Feng, F. Li, X. Li, X. Ren, D. Fan, D. Wu, H. Ma, B. Du, N. Zhang and Q. Wei, *J. Mater. Chem. B*, 7 (2019) 1142.
  43. J. Zhang, X. Zhang, Y. Gao, J. Yan and W. Song, *Biosens. Bioelectron.*, 176 (2021) 112945.